

# New Helical Complexes with a Bis(bidentate) Schiff Base Ligand Containing a Flexible Spacer

Miguel Vázquez,<sup>[a]</sup> Manuel R. Bermejo,<sup>\*[a]</sup> Matilde Fondo,<sup>[a]</sup> Ana García-Deibe,<sup>[a]</sup>  
Ana M. González,<sup>[a]</sup> and Rosa Pedrido<sup>[a]</sup>

**Keywords:** Supramolecular chemistry / Helical structures / Schiff bases / Electrochemistry

Neutral complexes with the general empirical formula  $M(\text{PTs})$  [ $M$ : Mn, Fe, Co, Cu, Zn, and Cd;  $\text{H}_2\text{PTs}$ :  $N,N'$ -bis(2-tosylaminobenzylidene)-1,3-diaminopropane] were obtained by means of an electrochemical procedure. All complexes were characterised by elemental analyses, mass spectrometry, IR and  $^1\text{H}$  NMR spectroscopy, and magnetic measurements, where appropriate. Recrystallisation of the cobalt, copper, and zinc complexes yielded single crystals of

$[\text{Co}(\text{PTs})]$  (**1**),  $[\text{Cu}(\text{PTs})]\cdot 1.5\text{CH}_3\text{CN}$  (**2**) and  $[\text{Zn}(\text{PTs})]_2\cdot 1.5\text{H}_2\text{O}\cdot \text{CH}_3\text{CN}$  (**3**). Their X-ray characterisation shows that **1** and **2** are mononuclear tetrahedral single-stranded helical complexes in the solid state, while **3** is a double-helical compound containing a major and a minor groove, with the Schiff base acting as a bis(bidentate)  $\text{N}_4$  donor.

## Introduction

The study of supramolecular helical complexes has been the subject of considerable interest recently, in order to clarify the mechanisms of self-assembly processes.<sup>[1–5]</sup> From these studies, it was concluded that metal helicates are generated by the combination of appropriate ligands and metal ions with specific preferences for particular coordination geometries.

Interesting studies have been devoted to the development of synthetic procedures, in order to prepare new multidentate ligands with the potential ability of forming bridged polynuclear species.<sup>[6–11]</sup> A key parameter in the assembly of helicates is how a flexible polydentate ligand becomes partitioned into distinct metal binding sites. In many cases ligands have been constructed that contain several bidentate or terdentate domains separated by rigid or bulky groups. Thus, the domains are arranged such that each site will definitely bind to different metal ions rather than chelating to a single metal centre. Furthermore, the spacer groups usually contain aromatic moieties, which provoke  $\pi\cdots\pi$  and/or  $\text{CH}\cdots\pi$  non-covalent interactions that control the self-assembly process.

The supramolecular chemistry involving ligands containing flexible spacers has not been extensively investigated. In this case, the way in which the ligand is partitioned into binding sites mainly depends on the stereoelectronic

preferences of the metal ion, and this type of ligand often leads to the isolation of mononuclear helical species.<sup>[12–14]</sup>

Our recent investigations on Schiff bases allowed us to isolate the bis(bidentate)  $\text{N}_4$  ligand  $\text{H}_2\text{PTs}$  [IUPAC name:  $N,N'$ -bis(2-tosylaminobenzylidene)-1,3-diaminopropane] (Scheme 1), which contains a flexible spacer. Its X-ray structure<sup>[15]</sup> shows that it adopts an *anti*-opened conformation<sup>[16]</sup> in the solid state that should do it suitable to span two metal centres, generating double-helical complexes. This is the situation found in the related  $[\text{Ni}(\text{PTs})]_2$  complex.<sup>[17]</sup> In an attempt to know the role of the metal atom in the disposition of this type of ligand, we extended our investigations to the behaviour of  $\text{H}_2\text{PTs}$ . In order to check if the arrangement of the ligand is the same as that found for nickel,<sup>[17]</sup> its electrochemical interaction with manganese, iron, cobalt, copper, zinc and cadmium was studied and the results obtained are described here.

## Results and Discussion

The Schiff base  $\text{H}_2\text{PTs}$  has been prepared as previously described and satisfactorily characterised by elemental analysis, FAB mass spectrometry, IR and  $^1\text{H}$  NMR spectroscopy,<sup>[17]</sup> and X-ray diffraction studies.<sup>[15]</sup>

### Synthesis of the Complexes

All the complexes were prepared by an electrochemical method previously described.<sup>[17,18]</sup> The electrochemical efficiency of the cell  $E_f$  was approximately  $0.5 \text{ mol}\cdot\text{F}^{-1}$  in all cases, which is compatible with the reaction mechanism shown in Scheme 2.

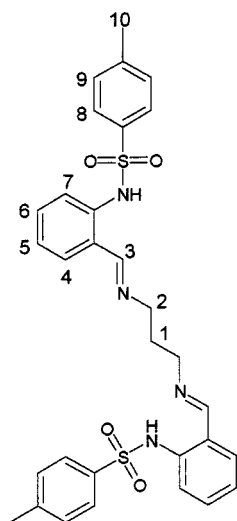
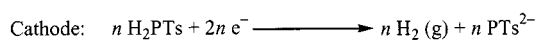
Elemental analyses (Table 1) show that all metal ions react with the ligand in a 1:1 molar ratio affording complexes

<sup>[a]</sup> Departamento de Química Inorgánica, Facultad de Química, Universidade de Santiago de Compostela, 15706 Santiago de Compostela, Spain  
Fax: (internat.) + 34-981/597-525  
E-mail: qimb45@usc.es

Table 1. Elemental analysis and some selected data for the complexes

Compound	Yield (%)	Colour	% C <sup>[a]</sup>	% H <sup>[a]</sup>	% N <sup>[a]</sup>	% S <sup>[a]</sup>	FAB <sup>[b]</sup>	$\mu$ <sup>[c]</sup>
Mn(PTs)	72	ochre	57.8 (58.0)	4.8 (4.7)	8.6 (8.7)	9.9 (10.0)	641	6.0
Fe(PTs)	65	red	57.9 (57.9)	4.6 (4.6)	8.6 (8.7)	9.7 (9.9)	642	5.1
Co(PTs)	70	garnet	57.8 (57.6)	4.4 (4.6)	8.7 (8.7)	9.6 (9.9)	646	4.3
Cu(PTs)	75	green	57.1 (57.2)	4.6 (4.6)	8.7 (8.6)	9.8 (9.8)	650	2.2
Zn(PTs)	81	yellow	56.9 (57.0)	4.8 (4.6)	8.4 (8.6)	9.9 (9.8)	651	
Cd(PTs)	77	yellow	53.4 (53.2)	4.1 (4.3)	7.7 (8.0)	9.0 (9.1)	701	

<sup>[a]</sup> Found (calculated). <sup>[b]</sup> amu; peaks corresponding to [ML]<sup>+</sup>. <sup>[c]</sup> In BM.

Scheme 1. H<sub>2</sub>PTs

$$n = 1, 2$$

Scheme 2

of the bis(deprotonated) ligand [PTs]<sup>2-</sup> in high purity. These neutral metal complexes are obtained in high yields and appear to be stable in the solid state and in solution. Most of them are insoluble or sparingly soluble in water and common organic solvents, but soluble in polar coordinating organic solvents such as DMF, DMSO, and pyridine.

## Crystal Structures

### [Co(PTs)] (1) and [Cu(PTs)]·1.5CH<sub>3</sub>CN (2)

The crystal structures of **1** and **2** are shown in Figures 1 and 2, respectively. Selected bond lengths and angles are displayed in Table 2.

Both compounds consist of discrete molecules of M(PTs) and show quite similar structures. In complex **2**, two acetonitrile solvates per complex molecule are present in the unit cell, one of them at 0.5 occupancy.

In both complexes, the ligand uses all its N-donor atoms to bind to the same metal centre. One oxygen atom of each

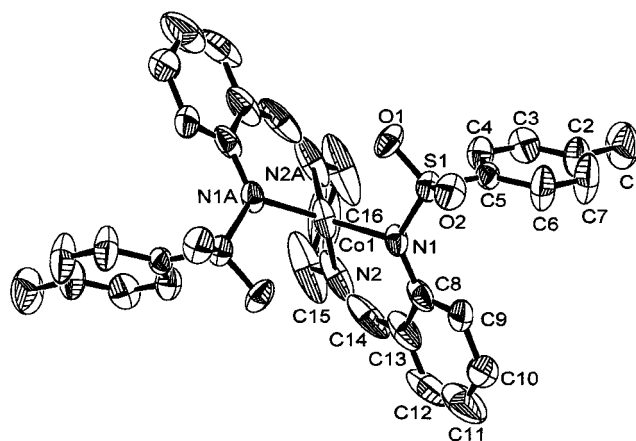


Figure 1. ORTEP view of complex **1** (thermal ellipsoids are drawn at 30% of probability level)

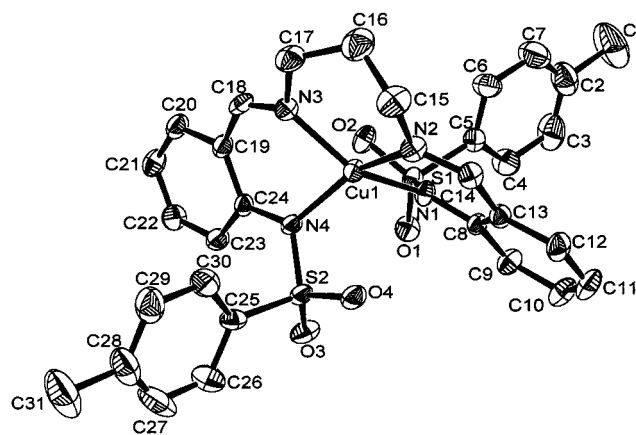


Figure 2. ORTEP view of complex **2** (thermal ellipsoids are drawn at 30% of probability level; hydrogen atoms and solvent molecules have been omitted for clarity)

tosyl group seems to weakly interact with the metal atom, the M...O distances (about 2.6 Å for **1** and 2.8 Å for **2**) are too long to be considered as true coordinated bonds, and therefore are best described as secondary intramolecular interactions. Thus, the metal centres are tetracoordinated, with the cobalt atom located in a twofold crystallographic axis in **1**. The geometry about the metal ions could be described as pseudo-tetrahedral, although the two terminal bidentate fragments are not mutually perpendicular. The dihedral angle  $\theta$  between the two MNN terminal planes is 69.38° for **1** and 44.37° for **2**. This shows that the deviation

Table 2. Selected bond lengths [Å] and angles [°] for **1**–**3**

1		2		3			
Co(1)–N(1)	1.962(6)	Cu(1)–N(1)	1.985(5)	Zn(1)–N(1)	1.985(6)	N(5)–Zn(1)–N(2)	106.4(2)
Co(1)–N(1A)	1.962(6)	Cu(1)–N(2)	1.973(5)	Zn(1)–N(2)	2.027(6)	N(1)–Zn(1)–N(6)	111.5(2)
Co(1)–N(2)	2.020(11)	Cu(1)–N(4)	1.975(5)	Zn(2)–N(3)	2.026(6)	N(5)–Zn(1)–N(6)	92.9(2)
Co(1)–N(2A)	2.020(11)	Cu(1)–N(3)	1.981(5)	Zn(2)–N(4)	1.971(6)	N(2)–Zn(1)–N(6)	103.8(2)
N(1)–Co(1)–N(1A)	128.6(3)	N(2)–Cu(1)–N(4)	149.7(2)	Zn(1)–N(5)	1.987(6)	N(8)–Zn(2)–N(4)	139.7(2)
N(1)–Co(1)–N(2)	89.0(4)	N(2)–Cu(1)–N(3)	97.9(2)	Zn(1)–N(6)	2.039(6)	N(8)–Zn(2)–N(3)	110.7(2)
N(1)–Co(1)–N(2A)	128.1(3)	N(4)–Cu(1)–N(3)	89.2(2)	Zn(2)–N(7)	2.027(5)	N(4)–Zn(2)–N(3)	94.5(2)
N(1A)–Co(1)–N(2)	128.1(3)	N(2)–Cu(1)–N(1)	89.7(2)	Zn(2)–N(8)	1.964(6)	N(8)–Zn(2)–N(7)	93.8(2)
N(1A)–Co(1)–N(2A)	89.0(4)	N(4)–Cu(1)–N(1)	99.4(2)	N(1)–Zn(1)–N(5)	144.6(2)	N(4)–Zn(2)–N(7)	108.0(2)
N(2)–Co(1)–N(2A)	92.6(8)	N(3)–Cu(1)–N(1)	148.7(2)	N(1)–Zn(1)–N(2)	92.7(2)	N(3)–Zn(2)–N(7)	108.2(2)

from tetrahedral to square-planar geometry is higher for the copper complex ( $\theta = 0$  for square-planar geometry and  $\theta = 90$  for tetrahedral geometry). The wide range of angles observed around the metal centres [from 89.0(4) to 128.1(3)° for **1** and from 89.2(2) to 149.7(2)° for **2**] also shows the deviation from the ideal tetrahedral geometry. The M–N distances are typical of cobalt and copper complexes with this type of ligand,<sup>[19–20]</sup> although it should be noted that all the Cu–N bonds are very similar while the Co–N<sub>amide</sub> bonds are significantly shorter than the Co–N<sub>imine</sub> bonds (Table 2).

The tetradentate dianionic Schiff base PTs<sup>2-</sup> wraps around the metal ions affording helical molecules in both cases. The screwed disposition of the ligand seems to be favoured by the presence of the two terminal bulky tosyl groups. The steric hindrance induced by these tosyl groups appears to provoke a twisting of the Schiff base, in order to minimise the steric interactions. Therefore, the torsion of the flexible spacer allows a remarkable shortening of the N<sub>imine</sub>...N<sub>imine</sub> distances relative to the free ligand (ca. 2.9 Å for **1** and **2**, and ca. 4.4 Å for free H<sub>2</sub>PTs<sup>[15]</sup>). This permits the four nitrogen atoms to bind to the same metal centre, leading to the isolation of mononuclear, tetrahedral, single-stranded helical complexes. These compounds can be also classified as saturated,<sup>[4]</sup> as the Schiff base fulfil the stereochemical requirements of the cobalt and copper atoms. Both right- (*P*) and left-handed (*M*) helices<sup>[4]</sup> can be simultaneously observed (in 50% yields) in the unit cell of **1** and **2**.

The PTs<sup>2-</sup> ligand forms three six-membered chelate rings. The angles between adjacent calculated chelate planes show the screwing of the thread. The degree of twisting is much smaller for the copper complex than for the cobalt complex (the angles between adjacent chelates for **1** is 55.67° and for **2** are 29.78 and 12.68°). Besides, in the crystal structure it can be clearly seen that when the tosyl groups are excluded, the wrapping angle is smaller than 360°. This angle is significantly higher for the copper complex than for the cobalt complex (264° for **1** and 305° for **2**), and this trend correlates with the ionic radius, as expected.

Finally, no specific  $\pi$ -stacking interactions (face-face or face-edge  $\pi$ - $\pi$ ) can be identified, either between the benzyldene binding moieties or between terminal tosyl aromatic

rings, which probably appear to be separated in order to minimise the steric hindrance.

### [Zn(PTs)]<sub>2</sub>·1.5H<sub>2</sub>O·CH<sub>3</sub>CN (**3**)

An ORTEP view of **3** is shown in Figure 3. Main bond lengths are shown in Table 2.

The unit cell of complex **3** consists of [Zn(PTs)]<sub>2</sub> discrete molecules, with lattice acetonitrile and disordered water. The complex is dinuclear and adopts an *anti*-opened conformation, with the Schiff bases acting as bis(bidentate) donors.<sup>[16]</sup> Its structure is quite similar to that of the related [Ni(PTs)]<sub>2</sub> complex.<sup>[17]</sup> Each Schiff base uses the amide and imine nitrogen atoms corresponding to one of its arms [N(1), N(2); N(5), N(6)] to bind to Zn(1), and the nitrogen donor atoms of the remaining arm [N(3), N(4); N(7), N(8)] to bind to the second zinc atom [Zn(2)]. One oxygen atom of each tosyl group weakly interacts with the metal centre [the Zn(1)···O(1), Zn(1)···O(6), Zn(2)···O(4) and Zn(2)···O(7) distances are ca. 2.6 Å]. These distances could be secondary intramolecular interactions, as seen in **1** and **2**, as well as in [Ni(PTs)]<sub>2</sub>.<sup>[17]</sup> Therefore, each zinc centre has a four-coordinated pseudo-tetrahedral environment, bound to two imine and two amide nitrogen atoms.

The two ligands wrap around the metal–metal axis giving rise to a double-stranded dinuclear helical compound with a Zn···Zn separation of ca. 6.031 Å. This distance compares fairly well with that observed in its analogue nickel complex,<sup>[17]</sup> but is clearly shorter than that found for dizinc complexes with bis(bidentate) ligands containing a propylene spacer (11.29 Å).<sup>[21]</sup> The wrapping angle of both strands is ca. 240°, and shows less helical coiling of the ligand than for mononuclear complexes. Both (*P,P*) and (*M,M*) isomers are present in the unit cell in 50% yields.

The ligands form two six-membered chelate rings, one around each metal atom, which are nearly planar. The dihedral angles between the two ZnNN planes around the same zinc centre are 84.77° for Zn(1) and 82.51° for Zn(2), indicating the deviation of the coordination polyhedron from the ideal geometry. All the distances and angles are in the expected range for distorted tetrahedral zinc(II) complexes with Schiff bases.<sup>[22–23]</sup> The variety of angles [ranging from 92.7(2) to 144.6(2)° for Zn(1) and from 93.8(2)

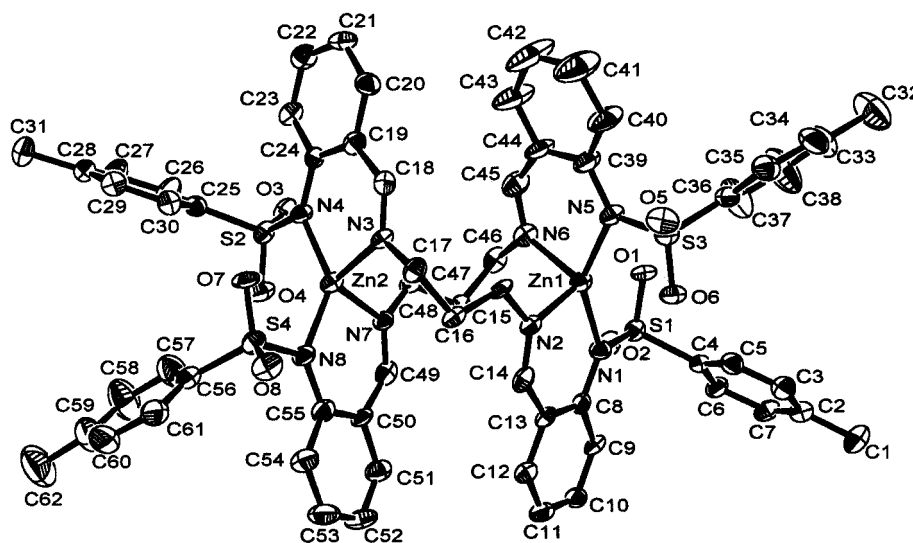


Figure 3. ORTEP view of complex **3** (thermal ellipsoids are drawn at 50% of probability level; hydrogen atoms and solvent molecules have been omitted for clarity)

to  $139.7(2)^\circ$  for Zn(2)] also show the distortion of the tetrahedral environment and that both metal atoms are not equivalent. All these features resemble those in the nickel analogue.<sup>[17]</sup> Besides, no symmetry elements relate the two ligands or the two halves of the same ligand. This leads to a certain degree of asymmetry in the complex, which gives rise to the formation of two different grooves (major and minor) (Figure 4), as seen in  $[\text{Ni}(\text{PTs})_2]_2$ .<sup>[17]</sup> In addition, no  $\pi$ -interactions are observed between the aromatic rings.

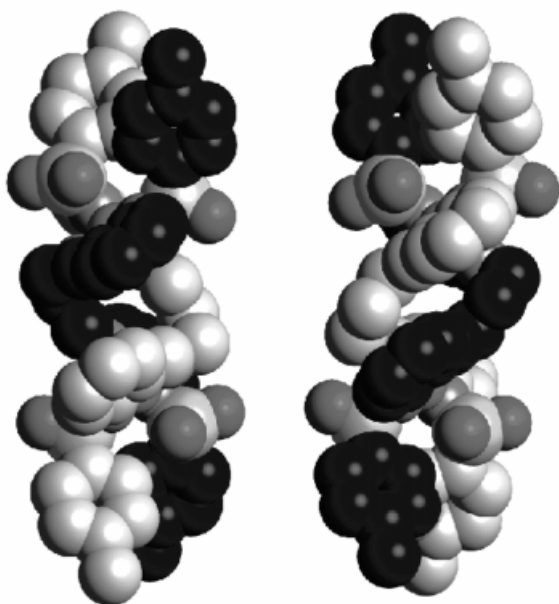


Figure 4. Space-filling representation of complex **1**, showing the minor (left) and major (right) grooves; both representations correspond to the same enantiomer, turned  $180^\circ$

In spite of the detailed NMR spectroscopic studies of van Koten on dinuclear zinc complexes with diimine ligands,<sup>[24]</sup> not many complexes of this kind have been reported. There

are some structurally characterised dizinc helical complexes described in the literature,<sup>[7,21,23–31]</sup> but only two helicates (one triple-stranded and one double-stranded) contain Schiff bases.<sup>[7,23]</sup> In these cases, the two bidentate domains are separated by a rigid spacer, which is the most general situation.<sup>[7,23,25–31]</sup> In fact, the structurally characterised zinc complexes derived from bis(bidentate) ligands containing flexible spacers are usually monohelical in the solid state,<sup>[13–14]</sup> and to the best of our knowledge, there are only two examples of bis(dipyrromethane)dizinc complexes with aliphatic spacers, where the extent of helicity is really small.<sup>[21]</sup> Therefore, the isolation of complex **3** further substantiates the NMR spectroscopic studies of van Koten and unequivocally demonstrates that Schiff bases with flexible spacers can generate zinc double-helical species.

#### IR Spectroscopy and FAB Mass Spectrometry

The IR spectra of all complexes show a strong band between  $1641$  and  $1612\text{ cm}^{-1}$  due to the imine  $\nu(\text{C}=\text{N})$  group (Table 3). This is a negative shift of  $4\text{--}23\text{ cm}^{-1}$  relative to the free ligand for all complexes except **3**. In the case of the zinc complex, the  $\nu(\text{C}=\text{N})$  band is shifted to higher wavenumbers ( $6\text{ cm}^{-1}$ ), indicating a slight shift of charge towards the CN group on coordination. However, the  $\nu(\text{C}-\text{N})$  stretching frequency is shifted to lower wave-

Table 3. Selected IR data for the complexes ( $\tilde{\nu}$ ,  $\text{cm}^{-1}$ )

Compound	$\nu(\text{C}=\text{N})$	$\nu(\text{C}-\text{N})$	$\nu_{\text{as}}(\text{SO}_2)$	$\nu_{\text{s}}(\text{SO}_2)$
$\text{H}_2\text{PTs}$	1635	1340	1287	1164
$\text{Mn}(\text{PTs})$	1624	1304	1272	1158
$\text{Fe}(\text{PTs})$	1612	1298	1260	1158
$\text{Co}(\text{PTs})$	1630	1296	1264	1134
$\text{Cu}(\text{PTs})$	1617	1297	1267	1137
$\text{Zn}(\text{PTs})$	1641	1296	1264	1137
$\text{Cd}(\text{PTs})$	1631	1294	1259	1128

Table 4. Selected  $^1\text{H}$  NMR chemical shifts ( $\delta$  values)

	H <sup>1</sup>	H <sup>2</sup>	H <sup>3</sup>	H <sup>5</sup>	H <sup>4</sup>	H <sup>7</sup>	H <sup>6</sup>	H <sup>9</sup>	H <sup>10</sup>	H <sup>8</sup>
H <sub>2</sub> PTs	2.07 (q, 2 H)	3.80 (t, 4 H)	8.55 (s, 2 H)	7.08 (t, 2 H)	7.48 (m, 4 H)		7.37 (t, 2 H)	7.27 (d, 2 H)	2.25 (s, 6 H)	7.65 (d, 2 H)
Zn(PTs)	2.17 (st, 2 H)	4.20, 3.88 (m, 4 H)	8.67 (s, 2 H)	6.93 (t, 2 H)	7.34 (d, 2 H)	7.50 (d, 2 H)		7.27 (m, 4 H)	2.32 (s, 6 H)	7.77 (d, 2 H)
Cd(PTs)	2.03 (b, 2 H)	3.80 (b, 4 H)	8.48 (s, 2 H)	6.86 (t, 2 H)	7.20 (d, 2 H)	7.38 (d, 2 H)		7.15 (m, 4 H)	2.27 (s, 6 H)	7.84 (d, 2 H)

numbers ( $36\text{--}46\text{ cm}^{-1}$ ) in all the complexes. This behaviour is compatible with the participation of both imine and amide nitrogen atoms in the coordination to the metal centres. In addition, two bands in the ranges  $1259\text{--}1272\text{ cm}^{-1}$  and  $1128\text{--}1158\text{ cm}^{-1}$  are assigned to the asymmetric and symmetric vibration modes of the  $\text{SO}_2$  group.<sup>[32–33]</sup> Finally, no bands above  $2500\text{ cm}^{-1}$  were detected for the complexes, indicating the deprotonation of the NH groups, and therefore the dianionic character of the ligand.

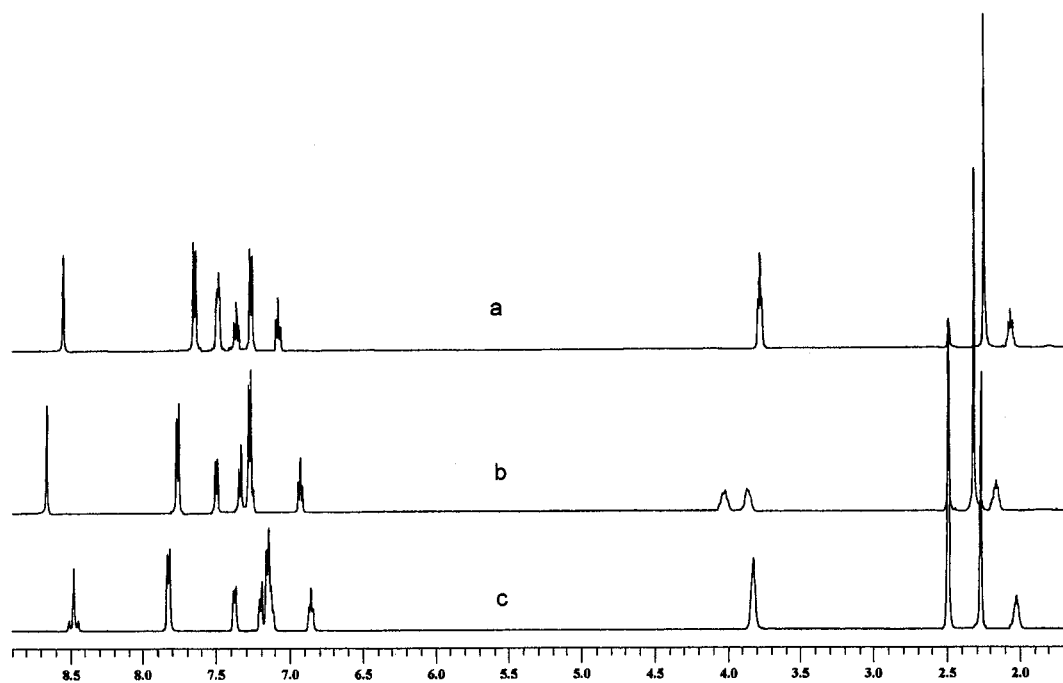
The FAB mass spectra show peaks assigned to the  $[\text{M}(\text{PTs})]^+$  fragments (Table 1) for all the complexes, indicating the coordination of the ligand to the metal centre. However, no other information about the nuclearity of the complexes can be drawn in this case study.

### $^1\text{H}$ NMR Spectroscopy

The  $^1\text{H}$  NMR spectra of the zinc and cadmium complexes were recorded in  $[\text{D}_6]\text{DMSO}$  as the solvent at room temperature (Table 4), and in  $\text{CD}_3\text{CN}$  at low temperatures (273 and 233 K). The spectra do not change significantly

with temperature. In fact, the spectra of the zinc complex recorded at the three different temperatures are identical. All spectra show a singlet set of proton resonances that could be fully assigned. This seems to indicate that there is a single species in solution. In all cases, the disappearance of the NH protons present in the free ligand is observed, which is in agreement with the bis(deprotonation) of the Schiff base. When the  $^1\text{H}$  NMR spectra of the free ligand is compared with those of the complexes at room temperature, some clear differences are observed (Figure 5):

1. The imine hydrogen atom (3-H) shows a downfield shift for the zinc complex, whilst it is displaced upfield in the spectrum of the cadmium complex, indicating that the coordination of the imine group to the metal centre induces opposite shielding effects on this hydrogen atom. Only one signal is observed for the H-imine atom in **3** at different temperatures suggesting that only symmetric species exist in solution. The imine protons of the cadmium complex are flanked by satellites arising from spin-spin coupling to  $^{111/113}\text{Cd}$ , indicating that the complex is kinetically inert on the NMR timescale.

Figure 5.  $^1\text{H}$  NMR spectra in  $[\text{D}_6]\text{DMSO}$  at room temperature for a)  $\text{H}_2\text{PTS}$ , b)  $\text{Zn}(\text{PTs})$ , and c)  $\text{Cd}(\text{PTs})$

2. The signals of the aromatic protons of the benzylidene ring are shifted upfield and the displacements are higher for the cadmium complex. The spectra show that complexation clearly affect the environments of 7-H and 4-H. In the spectra of the free ligand the signals are overlapped, while two sharp doublets are observed in the spectra of the complexes.

3. The signals of the aromatic protons of the tosyl groups also appear to be shifted on complexation, and the displacement is similar for the zinc and cadmium complexes.

4. Finally, the methylene protons of the cadmium and zinc complexes show different chiral behaviour in solution. The 2-H protons are equivalent in the free ligand and appear as a triplet at  $\delta = 3.80$ . However, for complex **3**, the 2-H protons appear as two multiplets at  $\delta = 3.88$  and 4.20. This implies that the strong coordination of the hard imine nitrogen atom to the zinc atom removes the erstwhile enantiotopic nature of the protons making them diastereotopic, and the complex chiral. This is also supported by the central methylene 1-H protons, which in the free ligand appear as a quintuplet at  $\delta = 2.07$ , while in **3** they appear as a septuplet at  $\delta = 2.17$  as a result of the coupling with two pairs of different protons. However, these central methylene hydrogen atoms seem to rotate freely as they are enantiotopic.

The spectrum of the cadmium complex is clearly different. Only one broad signal can be observed for the 2-H protons at room temperature, at  $\delta = 3.80$ . The 1-H protons also appear as a unique broad signal at  $\delta = 2.03$ . These signals get sharper on lowering the temperature, and a triplet (4 H) and a quintuplet (2 H) can clearly be observed for 2-H and 1-H, respectively. However, no splitting of the signal assigned to 2-H ( $\delta = 3.80$ ) is observed. This indicates that all 2-H protons are equivalent, in contrast to that found in **3**, and therefore that the cadmium complex is not chiral in solution.

### Magnetic Characterisation

Magnetic measurements at room temperature of all the paramagnetic compounds give similar values for the magnetic moments to those expected for magnetically diluted  $M^{II}$  ions. The magnetic moment of the manganese and copper complexes only allows for the confirmation of the +2 oxidation state for the central atom, indicating the deprotonation of the Schiff base ligand. The magnetic moments of Fe(PTs) and Co(PTs) are in agreement with high-spin  $M^{II}$  complexes. In both cases the magnetic moment is in the normal range for  $Fe^{II}$  (5.0–5.4 BM) and  $Co^{II}$  (4.3–4.8 BM) tetrahedral complexes. Thus, in view of the formulation of the complexes and their magnetic moments, it seems quite reasonable to propose a tetrahedral environment around the metal atom for all the paramagnetic complexes, as confirmed by the crystal structures of **1** and **2**.

Comparison of all the data obtained from the characterisation techniques employed herein with related complexes<sup>[17]</sup> leads us to conclude that zinc and nickel<sup>[17]</sup> form dinuclear double-stranded helicates, and Co and Cu yield mononuclear complexes with  $H_2PTs$  in the solid state. In addition, comparison of the  $^1H$  NMR spectroscopic data

of the Zn and Cd complexes seem to indicate that the tosyl groups behave in a similar way in both complexes and are not directly linked to the central atom, suggesting a tetrahedral environment for the metal centre in both cases. This tetrahedral environment can also be proposed for the other complexes on the basis of the magnetic measurements and X-ray results. Thus, the coordination preferences of the metal ion do not seem to have a profound effect on the disposition of the ligand and the nuclearity of the helix in this case study.

### Experimental Section

**General:** Elemental analysis was performed with a Carlo Erba EA 1108 analyser. The NMR spectra were recorded with a Bruker AMX-500 spectrometer using  $[D_6]DMSO$  (296 K) and  $CD_3CN$  (273 and 233 K) as solvents. Infrared spectra were recorded as KBr pellets with a Bio-Rad FTS 135 spectrophotometer in the range 4000–600  $cm^{-1}$ . Fast atom bombardment mass spectra (FAB) were obtained with a Kratos MS-50 mass spectrometer in *m*-nitrobenzyl alcohol as a matrix. Room-temperature magnetic measurements were performed using a Sherwood Scientific Magnetic Susceptibility Balance, calibrated using mercury tetrakis(isothiocyanato)cobaltate(II).

**Syntheses:** All the starting materials were purchased from Aldrich and used without further purification. 2-(Tosylamino)benzaldehyde was prepared according to literature methods<sup>[34]</sup> and was fully characterised.<sup>[35]</sup> *N,N'*-Bis(2-tosylaminobenzylidene)-1,3-diaminopropane ( $H_2PTs$ ) was synthesised as previously reported by us and characterised by elemental analyses, melting point, IR,  $^1H$  NMR spectroscopy and FAB mass spectroscopy and X-ray diffraction.<sup>[15,17]</sup>

**Synthesis of the Metal Complexes:** All complexes were prepared in a similar way, that can be exemplified by the isolation of  $[Co(PTs)]$  (**1**). A solution of  $H_2PTs$  (0.1 g, 0.15 mmol) in acetonitrile (80 mL), containing ca. 10 mg of tetramethylammonium perchlorate as the supporting electrolyte, was electrolysed for 1.8 h using a current of 5 mA. Concentration of the resultant solution to a third of its initial volume yielded a garnet solid that was washed with diethyl ether and dried in vacuo. Recrystallisation of the powder obtained in acetonitrile yielded single crystals of  $[Co(PTs)]$  (**1**), suitable for X-ray diffraction studies. The other complexes were obtained by the same method, using the appropriate metal anode. In the case of the manganese complex, the synthesis was performed in an inert gas under an argon stream. Recrystallisation of  $[Cu(PTs)]$  in acetonitrile and of  $[Zn(PTs)]$  by diffusion of ether into an acetonitrile solution, yielded crystals suitable for single X-ray analyses of  $[Cu(PTs)] \cdot 1.5CH_3CN$  (**2**) and  $[Zn(PTs)]_2 \cdot 1.5H_2O \cdot CH_3CN$  (**3**), respectively.

**CAUTION:** Perchlorate salts are potentially explosive and should therefore be handled with the appropriate care.

**X-ray Crystallography:** Crystals of **1** and **2**, suitable for X-ray diffraction studies, were grown as previously described. Data were collected at 298 K using a Siemens CCD diffractometer employing graphite-monochromated  $Mo-K\alpha$  ( $\lambda = 0.71073 \text{ \AA}$ ) radiation, using the  $\omega$ -scan mode. The structures were solved by direct methods<sup>[36]</sup> and refined by full-matrix least squares on  $F^2$ .<sup>[37]</sup> Absorption and incident beam corrections were applied (Sadabs). All non-hydrogen atoms were refined anisotropically. All hydrogen atoms were in-

Table 5. Crystal data and structure refinement

	1	2	3
Empirical formula	C <sub>31</sub> H <sub>30</sub> CoN <sub>4</sub> O <sub>4</sub> S <sub>2</sub>	C <sub>34</sub> H <sub>34.5</sub> CuN <sub>5.5</sub> O <sub>4</sub> S <sub>2</sub>	C <sub>64</sub> H <sub>66</sub> N <sub>9</sub> O <sub>9.5</sub> S <sub>4</sub> Zn <sub>2</sub>
Formula mass	654.64	711.83	1372.24
Crystal system	orthorhombic	monoclinic	monoclinic
Crystal size [mm]	0.40 × 0.20 × 0.15	0.50 × 0.4 × 0.25	0.30 × 0.25 × 0.25
a [Å]	9.292(3)	8.7453(4)	18.729(4)
b [Å]	26.518(13)	26.9760(12)	24.693(5)
c [Å]	12.458(3)	15.4879(6)	15.633(3)
α [°]	90	90	90
β [°]	90	101.1430(10)	107.097(10)
γ [°]	90	90	90
V [Å <sup>3</sup> ]	3069.8(20)	3584.9(3)	6910(2)
Space group	<i>Aba2</i> (no. 41)	<i>P21/n</i> (no. 14)	<i>P21/c</i> (no. 14)
Z	4	4	4
Absorption coefficient [mm <sup>-1</sup> ]	0.737	0.769	0.875
Reflections collected	6232	14814	20423
Independent reflections	2689 [ <i>R</i> <sub>int</sub> = 0.0375]	6312 [ <i>R</i> <sub>int</sub> = 0.0719]	12646 [ <i>R</i> <sub>int</sub> = 0.0608]
Final <i>R</i> indices [ <i>I</i> > 2σ( <i>I</i> )]	0.0504	0.0733	0.0713
<i>R</i> indices (all data)	0.0837	0.1239	0.1412

cluded in the model at geometrically calculated positions. Single crystals of **3** were grown as described above. Data were collected at 173 K using a Siemens CCD diffractometer employing graphite-monochromated Mo-*K*<sub>α</sub> (λ = 0.71073 Å) radiation, using the φ- and ω-scan mode. The structure was solved by direct methods and refined by full-matrix least squares on *F*<sup>2</sup>. Non-hydrogen atoms were refined anisotropically. All hydrogen atoms were included in calculated positions. Data processing and computation were carried out using the SHELX-97 program package.<sup>[38]</sup> Experimental details are shown in Table 5. Crystallographic data (excluding structure factors) for the structures reported in this paper have been deposited with the Cambridge Crystallographic Data Centre as supplementary publication nos. CCDC-166800 to -166802. Copies of the data can be obtained free of charge on application to CCDC, 12 Union Road, Cambridge CB2 1EZ, UK [Fax: (internat.) + 44-1223/336-033; E-mail: deposit@ccdc.cam.ac.uk].

## Acknowledgments

The authors thank the Xunta de Galicia (PGIDT99PXI20903B) and the Ministerio de Educación y Ciencia (Spain) (PB98-0600) for financial support. M. V. thanks the Fundación Segundo Gil Dávila for a grant.

[1] J. M. Lehn, *Supramolecular Chemistry-Concepts and Perspectives*, VCH, Weinheim, 1995.

[2] [2a] E. C. Constable, in: *Comprehensive Supramolecular Chemistry*, vol. 9 (Eds.: J. P. Sauvage, M. W. Hosseini), Pergamon Press, Oxford, 1996, p. 213–252. [2b] E. C. Constable, C. E. Housecroft, M. Neuburger, D. Phillips, P. R. Raithby, E. Schofield, E. Sparr, D. A. Tocher, M. Zehnder, Y. Zimmermann, *J. Chem. Soc., Dalton Trans.* 2000, 2219–2228.

[3] D. Philp, J. F. Stoddart, *Angew. Chem. Int. Ed. Engl.* 1996, 35, 1155–1196.

[4] C. Piguat, G. Bernardinelli, G. Hopfgartner, *Chem. Rev.* 1997, 97, 2005–2062.

[5] G. F. Swiegers, T. J. Malefse, *Chem. Rev.* 2000, 100, 3483–3537.

[6] [6a] M. J. Hannon, C. L. Painting, A. Jackson, J. Hamblin, W.

Errington, *Chem. Commun.* 1997, 1807–1808. [6b] N. W. Alcock, P. R. Barker, J. M. Haider, M. J. Hannon, C. L. Painting, Z. Pikramenou, E. A. Plummer, K. Rissanen, P. Saarenketo, *J. Chem. Soc., Dalton Trans.* 2000, 1447–1461. [6c] L. J. Childs, N. W. Alcock, M. J. Hannon, *Angew. Chem. Int. Ed.* 2001, 40, 1079–1081.

[7] N. Yoshida, K. Ichikawa, *Chem. Commun.* 1997, 1091–1092.

[8] C. R. Rice, S. Wörl, J. C. Jeffery, R. L. Paul, M. D. Ward, *J. Chem. Soc., Dalton Trans.* 2000, 550–559.

[9] H.-L. Zhu, Y.-X. Tong, X.-M. Cheng, *J. Chem. Soc., Dalton Trans.* 2000, 4182–4186.

[10] [10a] J. Sanmartín, M. R. Bermejo, A. García-Deibe, O. Piro, E. E. Castellano, *Chem. Commun.* 1999, 1953–1954. [10b] J. Sanmartín, M. R. Bermejo, A. M. García-Deibe, A. L. Llamas-Saiz, *Chem. Commun.* 2000, 795–796. [10c] O. L. Hoyos, M. R. Bermejo, M. Fondo, A. García-Deibe, A. M. González, M. Maneiro, R. Pedrido, *J. Chem. Soc., Dalton Trans.* 2000, 3122–3127.

[11] L. Carbonaro, M. Isola, V. Liuzzo, F. Marchetti, F. Balzano, C. S. Pomelli, A. Raffaelli, *Eur. J. Inorg. Chem.* 2001, 353–357.

[12] A. Jäntti, M. Wagner, R. Suontamo, E. Kolehmainen, K. Rissanen, *Eur. J. Inorg. Chem.* 1998, 1555–1562.

[13] S. C. Shoner, A. M. Nienstedt, J. J. Ellison, I. Y. Kung, D. Barnhart, J. A. Kovaks, *Inorg. Chem.* 1998, 37, 5721–5726.

[14] M. H. W. Lam, D. Y. K. Lee, S. S. M. Chiu, K. W. Man, W. T. Wong, *Eur. J. Inorg. Chem.* 2000, 1483–1488.

[15] J. Mahía, M. Maestro, M. Vázquez, M. R. Bermejo, J. Sanmartín, M. Maneiro, *Acta Crystallogr., Sect. C* 1999, 55, 1545–1546.

[16] N. Yoshida, H. Oshio, T. Ito, *J. Chem. Soc., Perkin Trans. 2* 1999, 975–983.

[17] M. Vázquez, M. R. Bermejo, M. Fondo, A. M. González, J. Mahía, L. Sorace, D. Gatteschi, *Eur. J. Inorg. Chem.* 2001, 1863–1868.

[18] C. Oldham, D. G. Tuck, *J. Chem. Educ.* 1982, 59, 420.

[19] A. Sousa, M. R. Bermejo, M. Fondo, A. García-Deibe, A. Sousa-Pedrares, O. Piro, *New J. Chem.* 2001, 25, 647–654.

[20] J. A. García-Vázquez, J. Romero, M. L. Durán, A. Sousa, A. D. Garnovskii, A. S. Burlov, D. A. Garnovskii, *Polyhedron* 1998, 17, 1547–1552.

[21] A. Thompson, D. Dolphin, *J. Org. Chem.* 2000, 65, 7870–7877.

[22] J. Romero, J. A. García-Vázquez, M. L. Durán, A. Castiñeiras,

- A. Sousa, A. D. Garnovskii, D. A. Garnovskii, *Acta Chem. Scand.* **1997**, *51*, 672–675.
- [23] N. Yoshida, K. Ichikawa, M. Shiro, *J. Chem. Soc., Perkin Trans. 2* **2000**, 17–26.
- [24] C. G. van Stein, G. van Koten, H. Passenier, O. Steinebach, K. Vrieze, *Inorg. Chim. Acta.* **1984**, *89*, 79–87.
- [25] G. Struckmeier, U. Thewalt, J. H. Furhop, *J. Am. Chem. Soc.* **1976**, *98*, 278–279.
- [26] D. Wester, G. J. Palenik, *Inorg. Chem.* **1976**, *15*, 755–761.
- [27] W. S. Sheldrick, J. Engel, *Acta Crystallogr., Sect. B* **1981**, *37*, 250–251.
- [28] C. Lorenzini, C. Pelizzi, G. Pelizzi, G. Predieri, *J. Chem. Soc., Dalton Trans.* **1983**, 2155–2158.
- [29] A. Bino, N. Cohen, *Inorg. Chim. Acta* **1993**, *210*, 11–16.
- [30] R. Chotalia, E. C. Constable, M. Neuburger, D. R. Smith, M. Zehnder, *J. Chem. Soc., Dalton Trans.* **1996**, 4207–4216.
- [31] Y. Zhang, A. Thompson, S. J. Rettig, D. Dolphin, *J. Am. Chem. Soc.* **1998**, *120*, 13537–13538.
- [32] M. Morioka, M. Kato, H. Yoshida, T. Ogata, *Heterocycles* **1997**, *45*, 1173–1181.
- [33] K. Nakamoto, in: *Infrared and Raman Spectra of Inorganic and Coordination Compounds*, John Wiley & Sons, New York, **1997**.
- [34] N. I. Chernova, Y. S. Ryabokobylky, V. G. Brudz, B. M. Bolotin, *Zh. Neorg. Khim.* **1971**, 1680–1687.
- [35] J. Mahía, M. Maestro, M. Vázquez, M. R. Bermejo, A. M. Gonzalez, M. Maneiro, *Acta Crystallogr., Sect. C* **1999**, *55*, 2158–2160.
- [36] G. M. Sheldrick, “SHELXS-86”, in: *Crystallographic Computing* (Eds.: G. M. Sheldrick, C. Krueger, R. Goddard), Oxford University Press, **1985**.
- [37] G. M. Sheldrick *SHELXL 93*, University of Göttingen, Germany, **1993**.
- [38] G. M. Sheldrick, *SHELX-97 (SHELXS 97 and SHELXL 97)*, *Programs for Crystal Structure Analyses*, University of Göttingen, Germany, **1998**.

Received July 12, 2001  
[I01263]